

This Page Is Inserted by IFW Operations
and is not a part of the Official Record

BEST AVAILABLE IMAGES

Defective images within this document are accurate representations of the original documents submitted by the applicant.

Defects in the images may include (but are not limited to):

- BLACK BORDERS
- TEXT CUT OFF AT TOP, BOTTOM OR SIDES
- FADED TEXT
- ILLEGIBLE TEXT
- SKEWED/SLANTED IMAGES
- COLORED PHOTOS
- BLACK OR VERY BLACK AND WHITE DARK PHOTOS
- GRAY SCALE DOCUMENTS

IMAGES ARE BEST AVAILABLE COPY.

**As rescanning documents *will not* correct images,
please do not report the images to the
Image Problem Mailbox.**

THIS PAGE BLANK (USPTO)

POWDER-MATERIAL RESEARCH METHODS AND PROPERTIES

POLYTERMAL SECTIONS OF THE $\text{Al}_2\text{O}_3-\text{ZrO}_2-\text{Y}_2\text{O}_3$ PHASE DIAGRAM

S. N. Lakiza, L. M. Lopato,
and I. E. Kir'yakova

UDC 546.31:621.641:831

Polythermal sections of the $\text{Al}_2\text{O}_3-\text{ZrO}_2-\text{Y}_2\text{O}_3$ phase diagram confirm that the system is quasibinary and enable one to give a complete phase diagram for the system. The ternary eutectic $\text{Al}_2\text{O}_3 + \text{ZrO}_2$ (solid solution) + $\text{Y}_3\text{Al}_5\text{O}_{12}$ has the lowest melting point in the system, whose temperature is 1715°C. No single-phase regions for the ternary solid solutions have been identified, which indicates that Al_2O_3 is not soluble in solid solutions based on F-ZrO_2 and $\text{C-Y}_2\text{O}_3$. This gives theoretical evidence for the scope for making new ceramics in this ternary system, which may have a high level of mechanical characteristics.

Materials in the $\text{Al}_2\text{O}_3-\text{ZrO}_2-\text{Y}_2\text{O}_3$ system have high values for the viscosity and strength in the family of high-technology ceramics. Elements of the phase diagram for this system have been researched in [1-7]. Data on the binary bounding systems have been taken from [8-21].

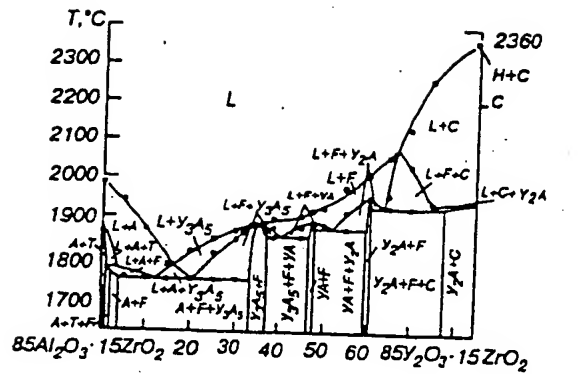
Our purpose was to construct polythermal sections of the $\text{Al}_2\text{O}_3-\text{ZrO}_2-\text{Y}_2\text{O}_3$ phase diagram in order to represent it more fully. We chose three sections: along the 15 mol. % ZrO_2 isoconcentrate (15Z); for 50 mol. % Al_2O_3 -50 mol. % ZrO_2 (50A·50Z)- Y_2O_3 ; and $\text{ZrO}_2-\text{YAlO}_3$ (YA). The initial substances and the experimental methods have been described in [5].

The 15Z isoconcentrate (Fig. 1) intersects four primary crystallization fields: those for the phases Al_2O_3 (A), $\text{Y}_3\text{Al}_5\text{O}_{12}$ (Y_3A_5) and for solid solutions based on the fluorite-type structure of ZrO_2 (F) with various Y_2O_3 (C). The solidus surface in the section is complicated. The section intersects five isothermal planes corresponding to one peritectic ($L_p + T \leftrightarrow F + A$, where T represents solid solutions based on the tetragonal form of ZrO_2 with various Y_2O_3 contents) and four eutectic ones ($L_{E1} \leftrightarrow \text{Y}_2\text{A} + F + C$, $L_{E2} \leftrightarrow \text{Y}_2\text{A} + F + YA$, $L_{E3} \leftrightarrow YA + F + \text{Y}_3\text{A}_5$, $L_{E4} \leftrightarrow \text{Y}_3\text{A}_5 + F + A$, where $\text{Y}_2\text{A} \leftrightarrow \text{Y}_4\text{Al}_2\text{O}_9$), which are nonvariant equilibria, and also lineated crystallization surfaces for six (out of eleven) binary eutectics: $L \leftrightarrow C + \text{Y}_2\text{A}$, $L \leftrightarrow \text{Y}_2\text{A} + F$, $L \leftrightarrow YA + F$, $L \leftrightarrow \text{Y}_3\text{A}_5 + F$, $L \leftrightarrow A + F$ and $L \leftrightarrow A + T$, whose crystallization volumes lie between the liquidus and solidus surfaces for the $\text{Al}_2\text{O}_3-\text{ZrO}_2-\text{Y}_2\text{O}_3$ system. The polymorphic transition in Y_2O_3 ($H \leftrightarrow C$) occurs at 2350°C, which is close to the eutectic in the $\text{ZrO}_2-\text{Y}_2\text{O}_3$ system (2360°C). The 15Z isoconcentrate intersects all three partially quasibinary sections in the ternary system, and the widths of the two-phase regions for these are seen in Fig. 1a.

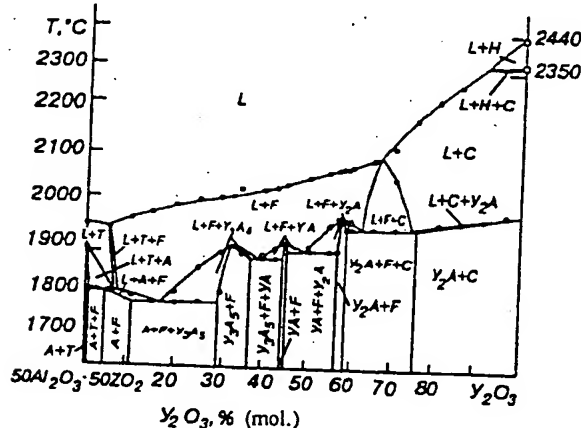
Parts a-c of Fig. 2 show heating curves for certain alloys in the 15 mol. % ZrO_2 isoconcentrate section, while Fig. 3 shows the microstructures.

The 50A·50Z- Y_2O_3 section intersects four primary crystallization fields: T, F, C, and H phases (Fig. 1b). The solidus surface is complicated, as is the 15 mol. % ZrO_2 isoconcentrate (Fig. 1a). The section intersects five isothermal planes corresponding to one peritectic nonvariant equilibrium P and four eutectic ones E_1 , E_2 , E_3 , and E_4 , and also lineated surfaces for the end of crystallization of the binary eutectics $C + \text{Y}_2\text{A}$, $\text{Y}_2\text{A} + F$, $YA + F$, $\text{Y}_3\text{A}_5 + F$, $A + F$. The A + T section between the liquidus and solidus surfaces in the ternary system intersects the crystallization volumes for eight binary eutectics: $L \leftrightarrow C + \text{Y}_2\text{A}$, $L \leftrightarrow \text{Y}_2\text{A} + F$, $L \leftrightarrow \text{Y}_3\text{A}_5 + F$, $L \leftrightarrow T + F$, $L \leftrightarrow F + C$, $L \leftrightarrow YA + F$, $L \leftrightarrow A + F$, $L \leftrightarrow T + A$.

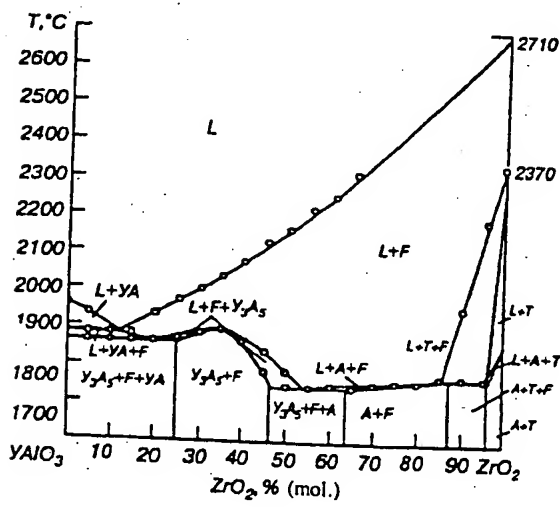
This section differs from the 15Z isoconcentrate section in that instead of the crystallization volume for the $\text{Y}_3\text{A}_5 + A$ binary eutectic it intersects the same volume for $T + F$. It is formed by connote triangles based on the equilibrium T and F phases, whose compositions lie near the ZrO_2 vertex and migrate along the curves $T'T''$ and $F'F''$, while the compositions of the liquid migrate along the monovariant equilibrium line m_2P [7], Fig. 1a. At the temperature of the peritectic four-phase



a



b



c

Fig. 1. Polythermal sections of the Al_2O_3 - ZrO_2 - Y_2O_3 phase diagram:
a) 15 ZrO_2 ; b) 50 Al_2O_3 -50 ZrO_2 - Y_2O_3 ; c) ZrO_2 - YAlO_3 .

equilibrium $\text{L}_p + \text{T} \leftrightarrow \text{F} + \text{A}$ (1745°C), the connode triangle lies in this plane and is part of it [7], region PT_2F_2 in Fig. 1a. Yttrium oxide undergoes a polymorphic transition at about 2350°C in a volume resembling a lobe in form and separating the solidus temperature, the section intersects three-phase regions separated by narrow two-phase regions, apart from the regions $\text{A} + \text{F}$ and $\text{Y}_3\text{A}_5 + \text{F}$, which have appreciable widths.

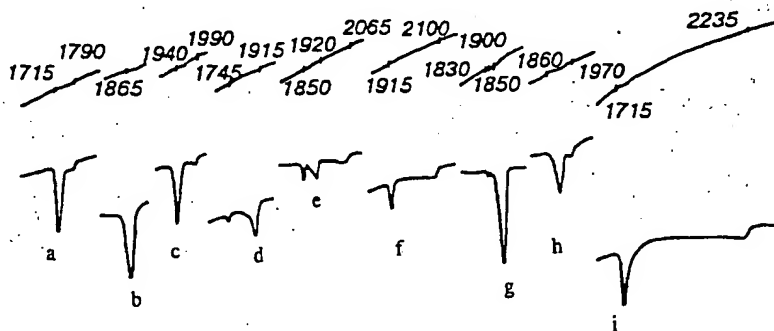


Fig. 2. Heating curves for alloys in polythermal sections of the $\text{Al}_2\text{O}_3-\text{ZrO}_2-\text{Y}_2\text{O}_3$ phase diagram. 15 ZrO_2 isoconcentrate: a) 20 Y_2O_3 ; b) 36 Y_2O_3 ; c) 60.5 Y_2O_3 . Section 50 $\text{Al}_2\text{O}_3\text{-}50 \text{ ZrO}_2\text{-}\text{Y}_2\text{O}_3$; d) 5 Y_2O_3 ; e) 55 Y_2O_3 ; f) 65 Y_2O_3 . Section $\text{ZrO}_2\text{-YAIO}_3$: g) 5 ZrO_2 ; h) 30 ZrO_2 ; i) 60 ZrO_2 .

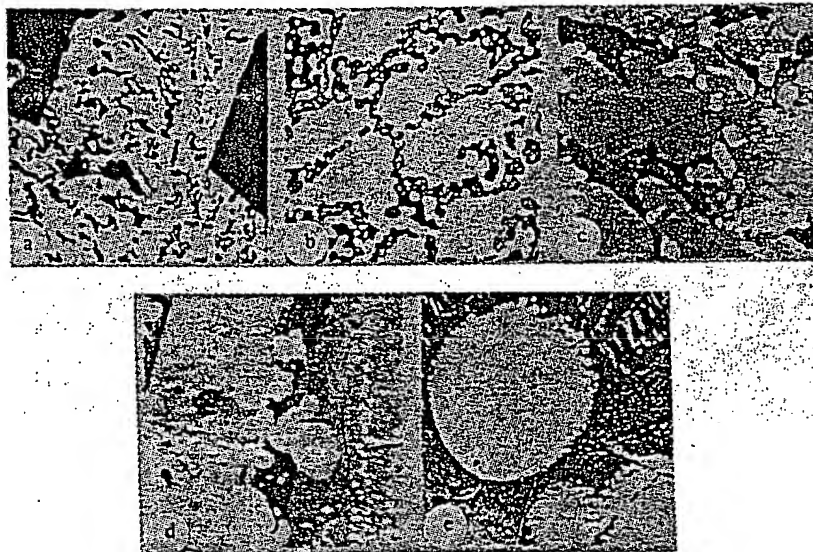


Fig. 3. Structure of alloys on the 15 ZrO_2 isoconcentrate for the $\text{Al}_2\text{O}_3-\text{ZrO}_2-\text{Y}_2\text{O}_3$ phase diagram. Y_2O_3 in mol. %: a) 15 (A, A + F + Y_3A_5); b) 20 (Y_3A_5 , A + F + Y_3A_5); c) 43 (F, F + YA, Y_3A_5 + F + YA); d) 56(F, F + Y_2A , YA + F + Y_2A); e) 70 (C, C + F, Y_2A + F + C); magnifications: a) 2000; b) 700; c and e) 1000; d) 800.

Parts d-f of Fig. 2 show heating curves for alloys in the 50A:50Z- Y_2O_3 section, while Fig. 4 shows the microstructures.

The $\text{ZrO}_2\text{-YA}$ section (Fig. 1c) indicates the structure of the $\text{Al}_2\text{O}_3\text{-ZrO}_2\text{-Y}_2\text{O}_3$ phase diagram at the ZrO_2 vertex. That section intersects two primary crystallization fields: YA and F. The solidus surface for this section is simpler than those for the two previous sections. The section intersects three isothermal planes corresponding to one peritectic nonvariant equilibrium P and two eutectic ones E_3 and E_4 , and also the linedated surfaces for the end of crystallization for the three binary eutectics Y_3A_5 + F, A + F and A + T, whose crystallization volumes lie between the liquidus and solidus surfaces in the $\text{Al}_2\text{O}_3\text{-ZrO}_2\text{-Y}_2\text{O}_3$ system. The temperature of the polymorphic transition in ZrO_2 ($\text{T} \leftrightarrow \text{F}$) falls smoothly as the Y_2O_3 content increases from 2370 to 1745°C, the temperature of the four-phase peritectic transformation $\text{L}_p + \text{T} \leftrightarrow \text{F} + \text{C}$. Below the solidus temperatures, the $\text{ZrO}_2\text{-YA}$ section intersects three three-phase regions separated by corresponding broad two-phase regions.

Parts g-i of Fig. 2 show the heating curves for certain alloys in the $\text{ZrO}_2\text{-YA}$ section, while Fig. 5 shows the microstructures.

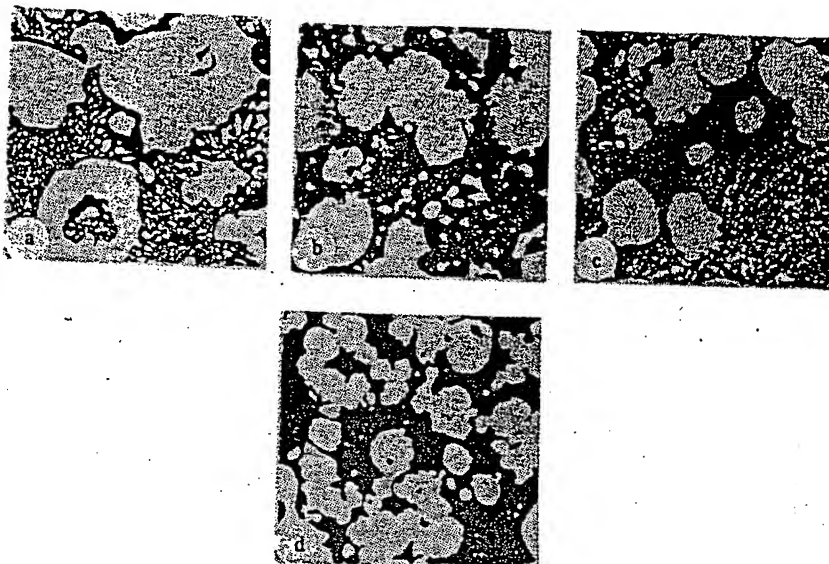


Fig. 4. Electron micrographs of certain alloys in the 50 Al_2O_3 -50 ZrO_2 - Y_2O_3 polythermal section for the Al_2O_3 - ZrO_2 - Y_2O_3 phase diagram, $\times 1000$. Y_2O_3 contents in mol. %: a) 3 (T, A + T + F); b) 12 (F, A + F, eutectic A + F + Y_3A_5); c) 20 (F, F + Y_3A_5 , A + F + Y_3A_5 eutectic); d) 65 (F, F + C, Y_2A + F + C eutectic).

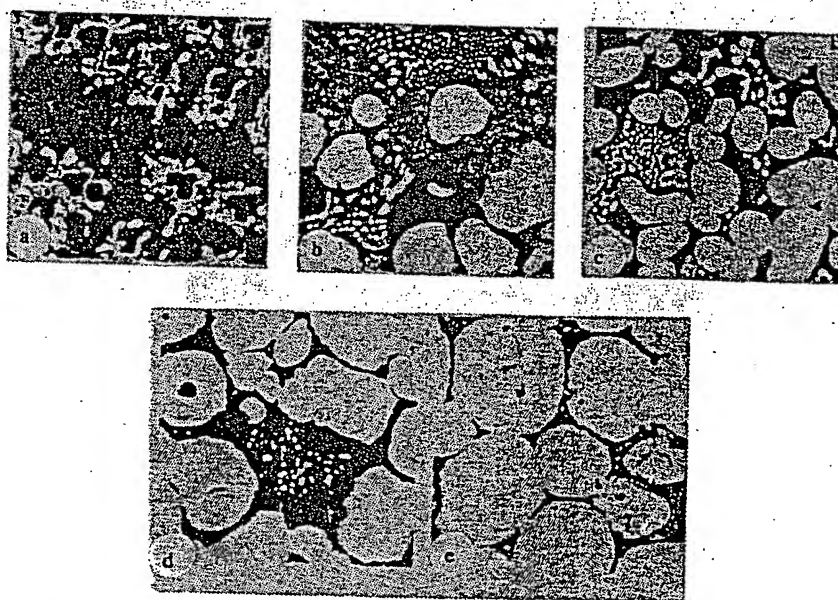


Fig. 5. Structures of alloys in the ZrO_2 - YAlO_3 polythermal section of the Al_2O_3 - ZrO_2 - Y_2O_3 phase diagram. ZrO_2 in mol. %: a) 10 (YA, YA + F, Y_3A_5 + F + YA); b) 22 (F, Y_3A_5 + F, Y_3A_5 + F + YA); c) 35 (F, Y_3A_5 + F); d) 60 (F, F + A, A + F + Y_3A_5); e) 80 (F, A + F). Magnifications: a) 600; b) 2000; c and d) 1000; e) 700.

These polythermal sections for the Al_2O_3 - ZrO_2 - Y_2O_3 system confirm that the sections examined in [5] are quasibinary. Together with the [5, 7] data, they give the complete phase diagram. The low melting point (1715°C) occurs for the Al_2O_3 + F + $\text{Y}_3\text{Al}_5\text{O}_{12}$ ternary eutectic. Single-phase regions for the ternary solid solutions are not observed, which shows that Al_2O_3 is not soluble in the F and C solid solutions. This is the theoretical basis for making new ceramics in this ternary system with a high level of mechanical properties.

REFERENCES

1. W. D. and T. Y. Tien, "Subsolidus phase equilibria in the $ZrO_2 - Y_2O_3 - Al_2O_3$ system," *J. Amer. Ceram. Soc.*, **63**, No. 9-10, 595-596 (1980).
2. S. G. Popov, S. F. Pashin, M. V. Paromova, et al., "Subsolidus phase equilibria in the $ZrO_2 - Y_2O_3 - Al_2O_3$ system," *Izv. AN SSSR, Neorgan. Mater.*, **26**, No. 1, 113-117 (1990).
3. L. M. Lopato, L. V. Nazarenko, G. I. Gerasimyuk, et al., "Interactions in the $ZrO_2 - Y_2O_3 - Al_2O_3$ system at 1650°C," *Ibid.*, No. 4, 834-838.
4. L. M. Lopato, L. V. Nazarenko, G. I. Gerasimyuk, et al., "The isothermal section of the $ZrO_2 - Y_2O_3 - Al_2O_3$ phase diagram at 1250°C," *Ibid.*, **28**, No. 4, 835-839 (1992).
5. S. N. Lakiza, L. M. Lopato, and A. V. Shevchenko, "Interactions in the $Al_2O_3 - ZrO_2 - Y_2O_3$ system," *Porosh. Metallurgiya*, No. 9-10, 46-51 (1994).
6. S. N. Lakiza, L. M. Lopato, L. V. Nazarenko, et al., "Liquidus surface for the $Al_2O_3 - ZrO_2 - Y_2O_3$ phase diagram," *Ibid.*, No. 11-12, 39-43.
7. S. N. Lakiza, L. M. Lopato, and V. P. Smirnov, "Solidus surface and phase equilibria in crystallization of alloys in the $Al_2O_3 - ZrO_2 - Y_2O_3$ system," *Ibid.*, No. 1-2, 71-76 (1995).
8. F. Schmid and D. Viechnicki, "Oriented eutectic microstructures in the system $Al_2O_3 - ZrO_2$," *J. Mater. Sci.*, **5**, No. 6, 470-473 (1970).
9. G. R. Fischer, L. J. Manfredo, R. N. McNally, et al., "The eutectic and liquidus in the $Al_2O_3 - ZrO_2$ system," *Ibid.*, **16**, No. 12, 3447-3451 (1981).
10. J. Echigoya, Y. Takabayashi, K. Sasaki, et al., "Solidification microstructure of Y_2O_3 -added $Al_2O_3 - ZrO_2$ eutectic," *Trans. Jap. Inst. Metals*, **27**, No. 2, 102-107 (1986).
11. A. V. Shevchenko, L. M. Lopatov, G. I. Gerasimyuk, et al., "The $HfO_2 - ZrO_2 - Al_2O_3$ system," *Izv. AN SSSR, Neorgan. Mater.*, **26**, No. 4, 839-842 (1990).
12. V. S. Stubican, R. G. Hink, and S. P. Ray, "Phase equilibrium and ordering in the system $ZrO_2 - Y_2O_3$," *J. Amer. Ceram. Soc.*, **61**, No. 1-2, 17-21 (1978).
13. A. V. Shevchenko, V. D. Tkachenko, L. M. Lopato, et al., "A method of determining phase-transition temperatures by the use of solar heating," *Porosh. Metallurgiya*, No. 1, 91-95 (1986).
14. A. V. Shevchenko, L. M. Lopato, T. V. Obolonchik, et al., "The liquidus surface in the $HfO_2 - ZrO_2 - Y_2O_3$ system," *Izv. AN SSSR, Neorgan. Mater.*, **23**, No. 3, 452-456 (1987).
15. N. A. Toropov, I. A. Bondar', F. Ya. Galakhov, et al., "Phase equilibria in the yttrium oxide-alumina system," *Izv. AN SSSR, Ser. Khim.*, No. 7, 1158-1164 (1964).
16. D. Viechnicki and F. Schmid, "Investigation of the eutectic point in the system $Al_2O_3 - Y_3Al_5O_{12}$," *Mater. Res. Bull.*, **4**, No. 2, 129-135 (1969).
17. J. L. Caslavski and D. J. Viechnicki, "Melting behavior and metastability of yttrium aluminium garnet (YAG) and $YAlO_3$ determined by optical differential thermal analysis," *J. Mater. Sci.*, **15**, No. 7, 1709-1718 (1980).
18. I. A. Bondar', L. N. Koroleva, and E. T. Bezruk, "Physicochemical properties of yttrium aluminates and gallates," *Izv. AN SSSR, Neorgan. Mater.*, **20**, No. 2, 257-261 (1984).
19. B. Cockayne, "The uses and enigmas of the $Al_2O_3 - Y_2O_3$ phase system," *J. Less-Common Met.*, **114**, No. 1, 199-206 (1985).
20. G. T. Adylov, G. V. Voronov, E. P. Mansurova, et al., "The $Y_2O_3 - Al_2O_3$ system above 1473 K," *Zh. Neorgan. Khimii*, **33**, No. 7, 1867-1869 (1988).
21. Tail-Ih Mah and M. D. Petry, "Eutectic composition in the pseudobinary system of $Y_4Al_2O_9$ and Y_2O_3 ," *J. Amer. Ceram. Soc.*, **75**, No. 7, 2006-2009 (1992).

THIS PAGE BLANK (C)